Correlation Coefficient Based DVB-T Continual Pilot Detection to Identify Spectrum Hole for CR Application

Mohammad Mizanur RAHMAN[1,2,*], Chalie CHAROENLARPNOPPARUT[2], Prapun SUKSOMPONG[2] and Attaphongse TAPARUGSSANAGORN[3]

[1]Electronics and Communication Engineering Discipline, Khulna University, Khulna, Bangladesh
[2]Electronics and Communication Engineering, Sirindhorn International Institute of Technology, Thammasat University, Bangkadi, Pathum Thani 12120, Thailand
[3]Wireless Information Security and Eco-Electronic Research Unit, National Electronics and Computer Technology Center, Thailand Science Park, Pathum Thani 12120, Thailand

([*]Corresponding author's e-mail: mizan.ku@gmail.com)

Received: 2 February 2015, Revised: 9 June 2015, Accepted: 28 July 2015

Abstract

Digital terrestrial television (DTV) covers an area with radius as large as 60 km. Federal Communications Commission (FCC) and Office of Communications (Ofcom) suggests detection of DTV signal at signal strength of as low as −114 dBm and −120 dBm respectively. Thus, detection of DTV signals in low signal-to-noise ratio (SNR) is vital. Continual pilot (CP) positions in all the DTV signals are fixed. Digital Video Broadcasting Terrestrial (DVB-T), a DTV standard, is followed by most of the countries of the world. In this paper we propose a correlation based CP detection which can detect a DVB-T signal at low SNR. One CP carrier was generated at the receiver which was correlated with the received orthogonal frequency division multiplexing (OFDM) signal sequence. The correlation coefficient was then compared with a threshold correlation coefficient to identify the existence of the CP to detect the presence of a DVB-T signal and thereby spectrum hole. It was found from the simulation study for additive white Gaussian noise (AWGN) channel that signal detection at low SNR is possible compared to the time domain symbol cross-correlation (TDSC) method.

Keywords: Cognitive radio, continual pilot, correlation coefficient, DVB-T, spectrum sensing

Introduction

Spatiotemporal underutilization of the frequency spectrum has been reported in a survey by the Federal Communications Commission (FCC) in 2004 [1]. Increasing the utilization of this valuable frequency spectrum can solve the present spectrum scarcity problem for wireless communications. The revolutionary concept of cognitive radio (CR) proposed by Mitola and Maguire [2] searches for spectrum holes in the allocated spectrum for different types of wireless services provided to licensed primary users (PUs) and utilizes the spatiotemporally free spectrum for efficient utilization of the spectrum. When a PU is activated, the CR system should detect it immediately and release that spectrum band and/or switch its operation to another available free band. Thus, detection of the presence of a PU is one of the most important tasks in CR systems.

Challenges faced by CR systems for spectrum sensing are: very low signal-to-noise ratio (SNR), channel uncertainty, fluctuating noise level with time, synchronization and so on. The simplest method to sense spectrum holes is energy detection (ED), which evaluates the energy of the received signal for detection [3,4]. Though ED is widely used in CR for its simplicity, it is not robust to the noise uncertainty and thus, this method is unreliable. Eigenvalue-based detection [5] improves the detection performance in the presence of noise uncertainty and outperforms the ED for highly correlated signals. The drawback for eigenvalue-based detection is that it cannot distinguish PU signals from interferences. Waveform-based detection studied in [6] exploits the waveform of transmitted signal to decide whether the intended PU is active. It was shown that the method achieves a perfect performance if *a priori* information about PU is enough. The cyclostationary feature detection method [7], which utilizes the cyclostationarity of the received signal, can meet the sensing requirements in CR without taking sensing time into account. FM channels operating in the TV bands has been shown to be detected at low SNR by an artificial neural network (ANN) based method which utilizes cyclostationary and SNR features as input parameters to the ANN [8].

Television transmission in America, Canada, European countries, and Australia has already switched to digital terrestrial television (DTV). Digital video broadcasting-terrestrial (DVB-T) which is popular in Europe with most of the countries in Asia using OFDM for transmission of DVB-T signal. The radius of coverage of DVB-T is about 60 km [9], which causes low signal strength and low SNR at the boundary. As a result sensing of OFDM signals at low SNR is of great importance for CR operation in DTV bands. One distinct feature of OFDM signals is in-band pilots multiplexed with data-carrying subcarriers. Utilization of pilot carriers for OFDM signal detection has got attention from researchers.

In-band sensing of OFDM signals without the quiet period needed for CR system exploiting complementary symbol couple (CSC) in a pilot signal has been proposed in [10]. In this paper the effect of the channel and self-signal of the network was eliminated by utilizing the complementary condition of OFDM symbols. The power detection was then performed over several OFDM frames. In this method the probability of detection varies with the number of observed frames for detection. However, its detection performance is limited since only a part of pilot symbols satisfies the complementary condition. An unsynchronized, random timing offset and carrier frequency offset robust sensing technique with the hybrid domain signal processing which matched the received OFDM signals with a local pilot reference was proposed in [11]. Timing average of the received OFDM signal segments was also done to improve the performance at low SNR. A detection probability of 0.9 was achieved in [12] by performing detection process over approximately 85 OFDM symbols. The methods proposed in [10-12] slow down the detection process as they require multiple OFDM symbols for sensing. In [13] a novel non-quiet PU detection scheme, which is based on pilot cancellation [14] of the CR transmitted known pilot signals is proposed. The performance of the proposed scheme was demonstrated only when the ED is applied. Compared to the detection scheme in [10], the scheme proposed in [13] can achieve better detection performance exploiting all OFDM symbols of pilot subcarriers for PU detection.

A novel spectrum sensing scheme for a DVB-T system proposed in [15], partitions the correlation values between the continual pilots (CP) and scattered pilots (SP) nearest to the CPs into several groups based on the sample distance between the CP and SP, and then eliminates the effect of timing synchronization error by re-correlating the correlation values in the same group. An algorithm which needs multiple OFDM symbols to detect spectrum hole into DVB-T spectrum by time domain autocorrelation of pilot signals presented in [16], is also able to differentiate single tone spurious with a DVB-T signal. A time domain symbol correlation (TDSC) method of spectrum hole identification is proposed in [17]. TDSC method chooses OFDM symbols in couples and their correlations are found. These correlations are averaged to find decision static. This method suffers from speed of detection as it employs multiple OFDM symbols for detection.

The goal for efficient detection of CR signals is to minimize the probability of misdetection and false alarm while maximizing the probability of detection. Misdetection probability is decreased if the threshold is lowered but it increases detection probability and false alarm probability. On the other hand false alarm probability can be reduced by increasing the threshold but it also decreases detection probability and increases misdetection probability. Our challenge is to find an optimal threshold to balance this dilemma. In addition the variation in channel noise and interference may also degrade the detection performance.

CPs and SPs are transmitted in DVB-T OFDM symbols with 4/3 times boosted amplitude compared to the data carriers. In addition CP positions are fixed in all DVB-T OFDM symbols [18]. When the noise power is as strong as data carriers, the CP carriers having higher power is expected to give higher SNR compared to data carriers and transmission parameter signal (TPS) carriers. In this paper we have used the correlation method to identify the existence of an expected CP into DVB-T signal and thereby made the detection decision. At the receiver a locally generated OFDM CP carrier of the target DVB-T band was generated and correlated to the received discrete time noisy signal. The correlation coefficient was then compared to the threshold correlation coefficient to identify the existence of the CP and thereby DVB-T PU signal. Detection performance of this method at different SNR level shows its capability to detect signals at low power and low SNR conditions.

Materials and methods

DVB-T OFDM system [18]

The DVB-T OFDM signal is organized in frames. Each frame has a duration T_F, and consists of 68 OFDM symbols indexed from 0 to 67. Four frames constitute one super-frame. Each symbol is constituted by a set of $K = 6817$ carriers in the 8K mode and $K = 1705$ carriers in the 2K mode and transmitted with a duration T_S. Here 8K stands for an 8192-points IFFT and 2K stands for a 2048-points IFFT. Transmission duration is composed of 2 parts: a useful part with duration T_U and a guard interval with a duration T_G. The guard interval consists in a cyclic continuation of the useful part, T_U, and is inserted before it. All symbols contain data and reference information. In addition to the transmitted data an OFDM frame contains.

Table 1 DVB-T OFDM 2K and 8K parameters.

Mode of operation		**2K**			**8K**		
Number of useful sub-Carriers, M		1705			6817		
Value of Carrier Number, K_{max}		1704			6816		
Value of Carrier Number, K_{min}		0			0		
Number of Continual Pilots (M_{cp})		45			177		
Number of Scattered Pilots (M_{sp})		141			564		
Spacing between carriers K_{min} and K_{max}, $\frac{K-1}{Tu}$ (MHz)		5.71	6.66	7.61	5.71	6.66	7.61
Bandwidth of RF channel, BW (MHz)		6	7	8	6	7	8
Elementary Period, $T = \frac{7}{8\text{BW}}$ (μs)		7/48	7/56	7/64	7/48	7/56	7/64
Symbol Duration, Tu (μs)		299	256	224	1195	1024	896
Sub-Carrier Spacing, $\frac{1}{Tu}$ (Hz)		3348	3906	4464	837	977	1116
Guard Interval, T_g	1/4	75 µs	64 µs	56 µs	299 µs	256 µs	224 µs
	1/8	37 µs	32 µs	28 µs	149 µs	128 µs	112 µs
	1/16	19 µs	16 µs	14 µs	75 µs	64 µs	56 µs
	1/32	9 µs	8 µs	7 µs	37 µs	32 µs	28 µs

Scattered pilot (SP): Inserted in every 12th subcarrier. The location of these pilot subcarriers are offset 3 subcarriers in consecutive DVB-T OFDM symbols. SPs repeat their pattern every 4 consecutive symbols.

CP carriers: Inserted in every OFDM symbol. 2K mode contains 45 CPs and 8K mode contains 177 CPs.

TPS carriers: Locations are constant and defined by the standard and all carriers convey the same information.

Table 1 shows the summary of the parameters of DVB-T OFDM 2K and 8K modes at a glance. The CPs in a 2K mode system are inserted according to the indices given in **Table 2**. The positions of CPs, SPs, and TPS in a transmission frame are shown in **Figure 1**. The pilots can be used for frame synchronization, frequency synchronization, time synchronization, channel estimation, transmission mode identification and can also be used to follow the phase noise. The CPs and SPs are modulated at a boosted power level, 4/3 times greater than that used for the data and TPS symbol carriers. The locations of the CPs are fixed for all the transmitted OFDM symbols.

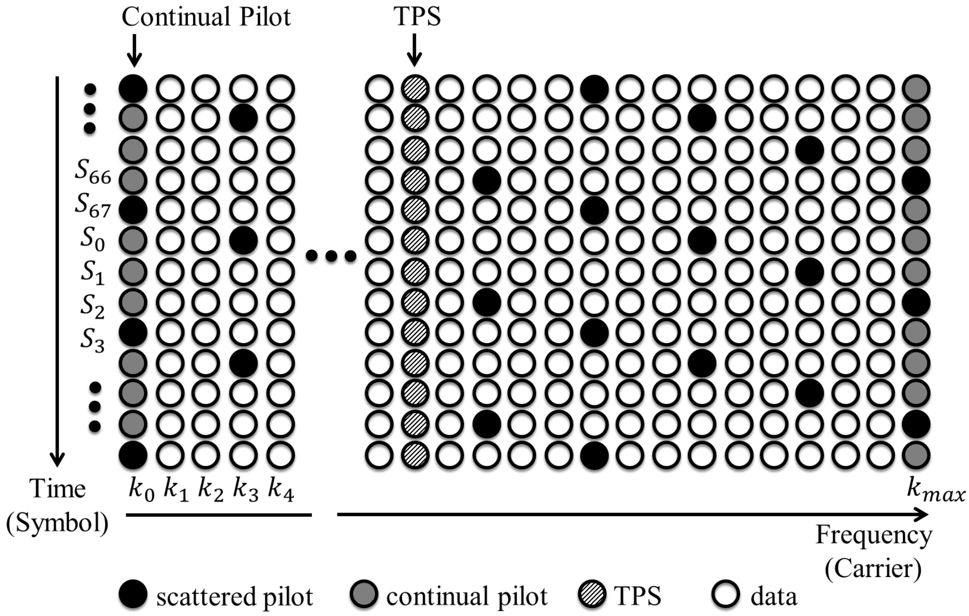

Figure 1 Transmission frame for the DVB-T 2K mode.

Table 2 Indices of continual pilot carriers in a DVB-T symbol for 2K mode.

0	**48**	**54**	**87**	**141**	**156**	**192**	**201**	**255**
279	282	333	432	450	483	525	531	618
636	714	759	765	780	804	873	888	918
939	942	969	984	1050	1101	1107	1110	1137
1140	1146	1206	1269	1323	1377	1491	1683	1704

It has been shown in [19] that the 2K mode is more suitable for mobile DVB-T reception due to the 4 times larger carrier-spacing it produces. In this paper, we realized one symbol of the DVB-T 2K system of European standard 8 MHz bandwidth by an inverse fast Fourier transform (IFFT) at the transmitter and a fast Fourier transform (FFT) at the receiver by taking DVB-T parameters into account as shown in **Table 1**.

DVB-T signal detection hypothesis

The primary goal of DVB-T spectrum sensing is to determine whether the DTV channel is occupied by a PU or is vacant. Determining a DVB-T signal on a specific spectrum band is categorized into a binary hypothesis problem, where, the null hypothesis H_0 corresponds to DVB-T signal absent and the alternative hypothesis H_1 corresponds to DVB-T signal present. These 2 hypotheses can be represented with the expressions as given in Eq. (1) below;

$$H_0: y(n) = w(n)$$
$$H_1: y(n) = x(n) + w(n) \tag{1}$$

where $x(n)$ is the DVB-T OFDM-based primary user signal including data signals $x_d(n)$ and pilot signals $x_p(n)$ which consist of the CPs and SPs. $y(n)$ represents the n^{th} sample of the received signal and $w(n)$ is the additive white Gaussian noise (AWGN) with a complex normal distribution $\mathcal{N}_c(0, \sigma_w^2)$.

TDSC method of DVB-T spectrum detection [16]

The decision statistic of the TDSC Neyman-Pearson (NP) test is given by Eq. (2) as follows;

$$T_{NP} = \left|\frac{1}{s_v}\sum_{m-l=v} R(l, m)\right|, \tag{2}$$

where s_v is the number of terms in correlation $R(l, m)$ that are accumulated and added, v is the symbol index difference of the 2 OFDM symbols.

For a single path channel the probability of misdetection is given as, $P_{md} = 1 - Q_{\chi_2'^2(\lambda)}\left(\frac{\tilde{a}^2}{\sigma_{H_1}^2}\right)$. The function $Q_{\chi_2'^2(\lambda)}(x) = \int_x^\infty \frac{1}{2} exp\left[\frac{-1}{2}(t+\lambda)\right] I_0\sqrt{\lambda t}\, dt$, is the right-tail probability of the non-central chi-squared distribution with 2 degrees of freedom, $\lambda = \left|\mu_{H_1}\right|^2/\sigma_1^2$ and γ is the threshold which is defined as, $\gamma = \sqrt{\sigma_{H_0}^2 ln\, P_{fa}}$, P_{fa} is the probability of false alarm. The function, $I_0(u) = \int_0^{2\pi} \exp\,(u\, cos\theta)\frac{d\theta}{2\pi}$ is the modified Bessel function of the first-kind and order zero, $\sigma_{H_0}^2$ and $\sigma_{H_1}^2$ are the variances of the distributions of the 2 hypothesis and μ_{H_1} is the mean of the distribution of the hypothesis H_1.

Proposed spectrum detection system model

We consider one symbol of a DVB-T OFDM 2K system with $\mathrm{M} = 1705$ sub-carriers, the high-speed binary serial input stream is denoted as $\{b_i\}$. After serial to parallel (S/P) conversion a new parallel signal sequence, $X = \{d_0, d_1, d_2, \dots, d_k, \dots, d_{M-1}\}$ is obtained. $\{d_k\}$ is considered to hold values from $\{0,1\}$ and when k is the CP index as shown in **Table 2**, $\{d_k\}$ holds the value from $\{1\}$. Each element of the parallel signal sequence is supplied to M orthogonal sub-carriers $\{e^{-i2\pi f_0 t}, e^{-i2\pi f_1 t}, \dots, e^{-i2\pi f_{M-1} t}\}$ for modulation, respectively. During modulation the CP and SP carriers are boosted 4/3 times compared to data carriers. Finally, modulated signals are added together to form an OFDM symbol. By IDFT complex envelope of the transmitted OFDM signals can be written as;

$$x(n) = \frac{1}{M}\sum_{k=0}^{K_{\max}} X_k e^{j2\pi f_k n},\ 0 \le n \le M-1, \tag{3}$$

where $f_k = k\Delta f$, Δf is sub-carrier spacing, and k is subcarrier index.

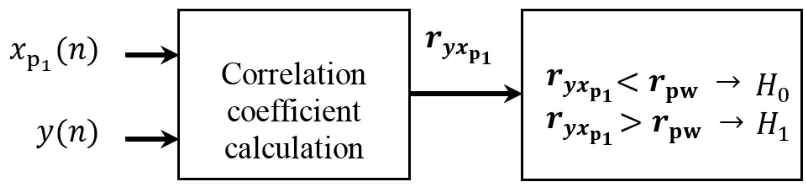

Figure 2 Block diagram of the DVB-T PU detector. r_{pw} is the detection threshold and $r_{yx_{p1}}$ is the correlation coefficient of $x_{p1}(n)$ correlated with $y(n)$.

The baseband representation of the signal received at the receiver is;

$$y(n) = x(n) + w(n), \tag{4}$$

where $w(n)$ is the AWGN and $x(n) = x_{\mathrm{p}}(n) + x_{\mathrm{d}}(n)$, and $n = 0,1,\dots,K_{max}$.

$$x(n) = \frac{1}{M}\left(\sum_{g\in A} X_{\mathrm{p}_g}(n)\left(\frac{4}{3}\right)e^{j2\pi f_g n} + \sum_{m\in B} X_{\mathrm{p}_m}(n)\left(\frac{4}{3}\right)e^{j2\pi f_m n} + \sum_{q\in C} X_{\mathrm{p}_q}(n)e^{j2\pi f_q n} + \sum_{v\in E} X_{\mathrm{d}_v}(n)e^{j2\pi f_v n}\right), \tag{5}$$

where A, B, C, and E are sets of CP indices, SP indices, TPS indices, and data carriers respectively. Thus by Eqs. (4) and (5);

$$y(n) = \frac{1}{M}\left(\begin{array}{c}\sum_{g\in A} X_{\mathrm{p}_g}(n)\left(\frac{4}{3}\right)e^{j2\pi f_g n} + \sum_{m\in B} X_{\mathrm{p}_m}(n)\left(\frac{4}{3}\right)e^{j2\pi f_m n} + \sum_{q\in C} X_{\mathrm{p}_q}(n)e^{j2\pi f_q n} \\ + \sum_{v\in E} X_{\mathrm{d}_v}(n)e^{j2\pi f_v n} + \sum_{k=0}^{K_{max}} W_k e^{j2\pi f_k n}\end{array}\right). \tag{6}$$

The generated pilot at the receiver is;

$$x_{\mathrm{p}_1}(n) = ae^{-j2\pi f_{\mathrm{p}_1} n}, \tag{7}$$

where a is the amplitude.
Correlation of $y(n)$ and $x_{\mathrm{p}_1}(n)$ as given in Eqs. (6) and (7) gives;

$$R_{yx_{\mathrm{p}_1}}(l) = \frac{1}{M}\sum_{n=0}^{M-1} y(n)\, ae^{-j2\pi f_{\mathrm{p}_1}(n-l)} \tag{8}$$

From Eq. (8);

$$R_{yx_{\mathrm{p}_1}}(l) = \frac{1}{M}\left(\frac{1}{M}\left(\begin{array}{c}\sum_{g\in A} X_{\mathrm{p}_g}(n)\left(\frac{4}{3}\right)e^{j2\pi f_g n} + \sum_{m\in B} X_{\mathrm{p}_m}(n)\left(\frac{4}{3}\right)e^{j2\pi f_m n} + \sum_{q\in C} X_{\mathrm{p}_q}(n)e^{j2\pi f_q n} + \\ \sum_{v\in E} X_{\mathrm{d}_v}(n)e^{j2\pi f_v n} + \sum_{k=0}^{K_{\max}} W_k e^{j2\pi f_k n}\end{array}\right) ae^{-j2\pi f_{\mathrm{p}_1}(n-l)}\right). \tag{9}$$

In the above Eq. (9) all the terms are cross-correlated except the generated CP carrier for which autocorrelation takes place and thus its contribution is significant in the above cross-correlation. The threshold r_{pw} in **Figure 2** was found from the general equation for correlation considering no signal was transmitted and only AWGN with a complex normal distribution $\mathcal{N}_c(0, \sigma_w^2)$ exists in the channel given as follows;

$$r_{\text{pw}} = \frac{E\left[\left(x_{\text{p}_1}(n) - \mu_{x_{\text{p}_1}}\right)(w(n) - \mu_w)\right]}{\sigma_{x_{\text{p}_1}} \sigma_w}, \tag{10}$$

where $\mu_{x_{p_1}}$ and μ_w are the mean of the generated pilot carrier at the receiver and mean of AWGN accordingly. Mean of the generated pilot carrier, $\mu_{x_{p_1}}$ was considered zero as sinusoidal signals results zero mean over full cycles. $\sigma_{x_{p_1}}$ and σ_w are standard deviation of the sinusoidal pilot carrier at the receiver and AWGN accordingly. For the sinusoidal pilot carrier $\sigma_{x_{p_1}}$ is given by, $\sigma_{x_{p_1}} = x_{rms} = \sqrt{\frac{1}{N}\sum_{n=1}^{N}[x(n)]^2}$, and $\sigma_w = 1$ is considered in our experiment for AWGN.

Thus from Eq. (10) we get, $r_{\text{pw}} = \frac{E\left[\left(x_{\text{p}_1}(n)\right)(w(n))\right]}{x_{rms}}$. The ideal value of the numerator is equal to zero as the expected value of a multiplication between a deterministic signal of mean zero and random Gaussian noise whose mean is also zero becomes Gaussian with zero mean. Thus we get, $r_{\text{pw}} = 0$. For precision inaccuracy the coefficient is not exactly zero but a very small value, and varies with the number of data samples considered. **Figure 3** represents the effect of the number of samples on the distribution of the correlation coefficient. The distribution of the correlation coefficient is given as a function of the correlation coefficient, r as in Eq. (11) [20].

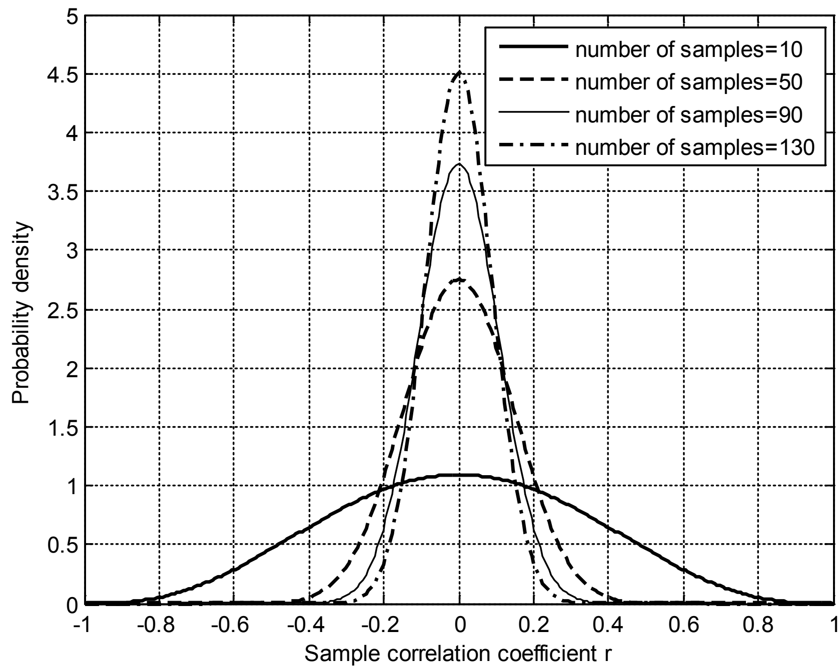

Figure 3 Sampling distribution of correlation coefficient *r*.

$$f(r) = \frac{(N-2)\Gamma(N-1)(1-\rho^2)^{(N-1)/2}(1-r^2)^{(N-4)/2}}{\sqrt{2\pi}\Gamma\left(N-\frac{1}{2}\right)(1-\rho r)^{N-3/2}}\left[1+\frac{1}{4}\frac{\rho r+1}{2N-1}+\frac{9}{16}\frac{(\rho r+1)^2}{(2N-1)(2N+1)}+\cdots\right], \quad (11)$$

where $\Gamma(\cdot)$ is the gamma function defined as, $\Gamma(N) = (N-1)!$, r represents the sample correlation, and ρ represents the population correlation.

It is seen from the distribution in **Figure 3** that the correlation distribution curve becomes steep representing the improvement of accuracy over the expected value of correlation with an increase in the number of samples. For the experiment we correlate the generated sinusoidal carrier with AWGN noise $10{,}000$ times and choose the 9000^{th} maximum correlation value from the minimum as the threshold to maintain the detection probability to 0.9 and false alarm rate to 0.1 which was found to be $r_{\mathrm{pw}} = 0.0035$. The threshold r_{pw} shall be changed depending on the required false alarm rate. In our experiment the probability of false alarm, the probability of detection and the probability of misdetection are defined as, $P_{\mathrm{fa}} = P\left(\left(r_{yx_{\mathrm{p}_1}} > r_{pw}\right)|H_0\right)$, $P_{\mathrm{d}} = P\left(\left(r_{yx_{\mathrm{p}_1}} > r_{\mathrm{pw}}\right)|H_1\right)$, and $P_{\mathrm{md}} = P\left(\left(r_{yx_{\mathrm{p}_1}} < r_{\mathrm{pw}}\right)|H_1\right)$ accordingly.

Results and discussion

The simulation study was done at different levels of SNR. Different signal strengths were chosen to keep track of FCC and Ofcom prescribed minimum signal level and corresponding SNR. AWGN was fixed to zero mean and one standard deviation throughout the experiment. **Table 3** shows the signal power in dBm, corresponding SNR in dB, and false alarm rate at different values of correlation threshold r_{pw}. It can be seen from **Table 3** that the probability of false alarm increases as the detection threshold r_{pw} is decreased but remains approximately invariant at different SNR values.

Table 3 False alarm rate for different SNR and signal power at different levels of threshold, r_{pw} and AWGN of $\mathcal{N}_c(0,1)$.

Signal power (dBm)	SNR (dB)	Probability of false alarm for correlation Threshold, r_{pw}		
		0.0035	0.003	0.0026
–66.65	–96.65	0.02	0.11	0.20
–60.63	–90.63	0.03	0.08	0.22
–57.10	–87.10	0.03	0.08	0.21
–51.09	–81.09	0.03	0.09	0.30
–49.74	–79.74	0.03	0.06	0.23
–46.65	–76.65	0.03	0.12	0.21

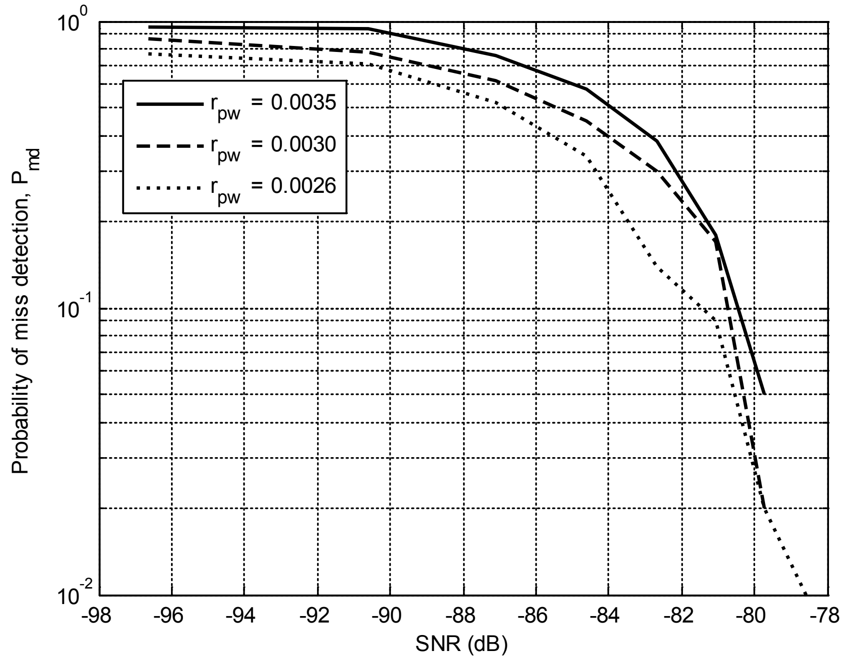

Figure 4 Probability of misdetection for different values of correlation threshold r_{pw}.

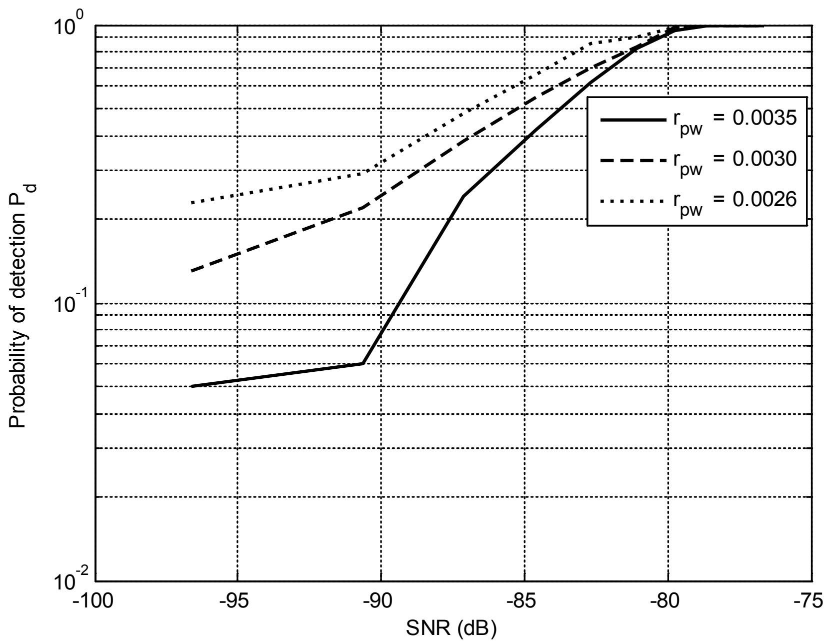

Figure 5 Probability of detection for different values of correlation threshold, r_{pw}.

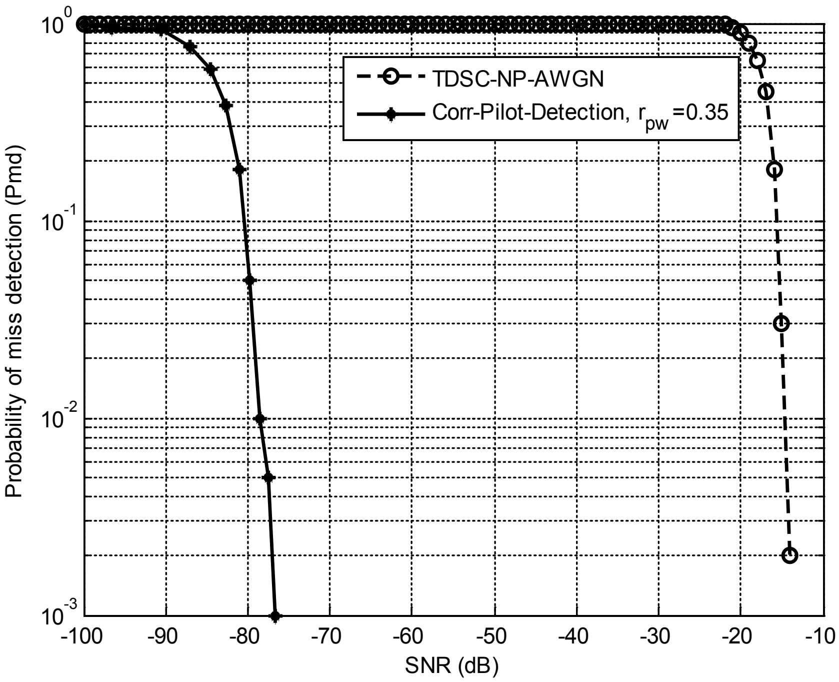

Figure 6 Comparison of the correlation based method to the TDSC-NP-AWGN method of detection.

Figures 4 and **5** depict the SNR versus the probability of misdetection and the probability of detection curves at 3 values of r_{pw}. As can be seen the probability of misdetection increases and the probability of detection decreases with an increase in the threshold correlation coefficient r_{pw}. From **Figure 4** we can see that at SNR of −90 dB the probability of misdetection is 0.9 for $r_{pw} = 0.0035$. In addition the probability of misdetection decreases as threshold decreases. From **Figure 5** it is marked that the probability of detection, $P_d = 0.9$ and 0.99 at SNR of approximately −81 dB and −79 dB correspondingly. From **Table 3** the signal strength that corresponds to –81 dB and –79 dB of SNR are –51.09 dBm and –49.74 dBm approximately. The false alarm rate at the corresponding SNR values is 0.03 which is much below the required false alarm rate of 0.1.

Figure 6 shows a comparative study of the proposed correlation coefficient based CP detection method to NP based TDSC detection method for AWGN channel (TDSC-NP-AWGN [16]) in terms of the probability of misdetection. For TDSC method $P_{\mathrm{md}} = 0.9$ at SNR -22 dB. The probability of misdetection of 0.1 can be seen at SNR − 81 dB and − 15 dB for the proposed correlation based on the CP detection and TDSC-NP-AWGN methods accordingly. This result shows the possibility of using the proposed correlation based CP detection method in CR communications where detection is required at low signal strength and low SNR.

Conclusions

A correlation based DVB-T signal detection method was proposed in this paper where the received signal is correlated to a generated known CP. It was found that this method can detect signals efficiently in low SNR and at very low signal levels. The proposed method requires only one symbol to be received and correlated to the generated carrier. As expected this method can speed up the detection process if implemented as it senses the channel for one OFDM symbol duration and needs to process fewer samples compared to the cases where sensing is performed over multiple symbols or multiple frames. An open loop analysis was performed in this paper. For future works the authors plan to investigate a closed loop analysis of the proposed method on different channel conditions.

Acknowledgements

The authors thank the Thailand Research Fund (TRF) and the Thailand Office of Higher Education Commission (NRU Project) for their financial support.

References

[1] Federal Communications Commission. *Notice of Proposed Rulemaking FCC04-113: Unlicensed Operation in the TV Broadcast Bands*. Washington DC, USA, 2004.
[2] J Mitola and GQ Maguire. Cognitive radio: Making software radios more personal. *IEEE Pers. Commun*. 1999; **6**, 13-8.
[3] H Urkowitz. Energy detection of unknown deterministic signals. *Proc. IEEE* 1967; **55**, 523-31.
[4] FF Digham, MS Alouini and MK Simon. On the energy detection of unknown signals over fading channels. *IEEE Trans. Commun*. 2007; **55**, 21-4.
[5] D Cabric, A Tkachenko and RW Brodersen. Spectrum sensing measurements of pilot, energy, and collaborative detection. *In*: Proceedings of the IEEE Military Communications Conference 2006, Washington DC, USA, 2006, p. 1-7.
[6] M Kim, K Po and JI Takada. Performance Enhancement of cyclostationarity detector by utilizing multiple cyclic frequencies of OFDM signals. *In*: Proceeding of the IEEE Symposium on New Frontiers in Dynamic Spectrum, Singapore, 2010, p. 1-8.
[7] Z Yonghong and L Ying-Chang, Eigenvalue-based spectrum sensing algorithms for cognitive radio. *IEEE Trans. Commun*. 2009; **57**, 1784-93.
[8] S Pattanayak, R Nandi and P Venkateswaran. Identification of spectrum holes using ANN model in TV bands with AWGN. *In*: Proceedings of the IEEE Asia Pacific Conference on Wireless and Mobile 2014, Bali, Indonesia, 2014, p. 188-93.
[9] D Chen, J Li and J Ma. In-band sensing without quiet period in cognitive radio. *In*: Proceedings of the IEEE Wireless Communications and Networking Conference 2008, Las Vegas, USA, 2008, p. 723-8.
[10] DG Jeong, SS Jeong and WS Jeon. Channel sensing without quiet period for cognitive radio systems: A pilot cancellation approach. *EURASIP J. Wirel. Commun. Network.* 2011; **2011**, 650619.
[11] S Moshavi, D Yellin, JS Sadowsky, Y Perets and K Pick. Pilot interference cancellation technology for CDMA cellular networks. *IEEE Trans. Veh. Tech*. 2005; **54**, 1781-92.
[12] HW Chen, X Wang, CL Wang and H Lin. Spectrum sensing of unsynchronized OFDM signals for cognitive radio communications. *In*: Proceedings of IEEE 70th Vehicular Technology Conference Fall, Anchorage, USA, 2009, p. 1-5.
[13] XD Yang, YH Song, TJ Owens, J Cosmas and T Itagaki. Performance analysis of the OFDM scheme in DVB-T. *In*: Proceedings of the IEEE 6th Circuits and Systems Symposium on Emerging Technologies: Frontiers of Mobile and Wireless Communication, Shanghai, China, 2004, p. 489-92.
[14] D Tian, L Zheng, J Wang and L Zhao. A new spectrum sensing method for OFDM-based cognitive radios. *In*: Proceedings of the IEEE 2nd International Conference on Consumer Electronics, Communications and Networks, Yichang, China, 2012, p. 812-5.
[15] R Mo, SW Oh and B Wang. Spectrum sensing for DVB-T signals employing pilot tones. *In*: Proceedings of the IEEE Vehicular Technology Conference, Quebec City, Canada, 2012, p. 1-5.
[16] HW Cho, Y Lee, SG Kang, D Chong, M Lee, C Song and S Yoon. A novel spectrum sensing scheme based on periodicity of DVB-T pilot signals. *World Acad. Sci. Eng. Tech*. 2010; **4**, 580-4.
[17] HS Chen, W Gao and DG Daut. Spectrum sensing for OFDM systems employing pilot tones and application to DVB-T OFDM. *In*: Proceedings of the IEEE International Conference on Communications, Beijing, China, 2008, p. 3421-6.

[18] ETSI EN 300 744. *Digital Video Broadcasting (DVB); Framing Structure, Channel Coding and Modulation for Digital Terrestrial Television*. European Telecommunications Standards Institute, Valbonne, France, 2009.
[19] U Reimers. *Digital Video Broadcasting (DVB): The International Standard for Digital Television*. 1st ed. Springer-Verlag Berlin Heidelberg, New York, 2001, p. 335-8.
[20] Wolfram MathWorld, Available at: http://mathworld.wolfram.com/CorrelationCoefficientBivariateNormalDistribution.html, accessed February 2015.